

Telling tails in the presence of a cosmological constant

Patrick R. Brady,¹ Chris M. Chambers,² William Krivan,^{3,4} and Pablo Laguna⁴

¹ *Theoretical Astrophysics, Mail-Code 130-33, California Institute of Technology, Pasadena, California 91125*

² *Department of Physics, Montana State University, Bozeman, Montana 59717*

³ *Institut für Astronomie und Astrophysik, Universität Tübingen, D-72076 Tübingen, Germany*

⁴ *Department of Astronomy & Astrophysics and Center for Gravitational Physics & Geometry, Pennsylvania State University, University Park, Pennsylvania 16802*

(Received 15 November 1996; revised manuscript received 11 March 1997)

We study the evolution of massless scalar waves propagating on spherically symmetric spacetimes with a nonzero cosmological constant. Considering test fields on both Schwarzschild–de Sitter and Reissner–Nordström–de Sitter backgrounds, we demonstrate the existence of *exponentially* decaying tails at late times. Interestingly, the $\ell=0$ mode asymptotes to a nonzero value, contrasting the asymptotically flat situation. We also compare these results, for $\ell=0$, with a numerical integration of the Einstein-scalar field equations, finding good agreement between the two. Finally, the significance of these results to the study of the Cauchy horizon stability in black-hole–de Sitter spacetimes is discussed. [S0556-2821(97)06812-4]

PACS number(s): 04.30.Nk, 04.25.Dm, 04.70.Bw

I. INTRODUCTION

Perturbative studies of relativistic, spherical collapse have elucidated dynamical features of gravitational collapse important to our understanding of black-hole formation, and the subsequent relaxation to a stationary state (see [1], for example). Indeed, quasinormal ringing could provide direct evidence of the existence of black holes if observed by the Laser Interferometric Gravitational Wave Observatory (LIGO) [2]. At late times, quasinormal oscillations are swamped by the radiative tail of the gravitational collapse [3]. This tail radiation is of interest in its own right since it originates from the nontrivial propagation of the field perturbations on the background spacetime, zero rest-mass fields do not necessarily propagate along the light cone in a curved spacetime.

The first authoritative study of nearly spherical collapse, exhibiting radiative tails, was performed by Price [3]. Studying the behavior of a massless scalar field propagating on a fixed Schwarzschild background, he showed that the field dies off with the now familiar power-law tail $t^{-(2\ell+P+1)}$, at late times, where ℓ is the multipole order of the field, and $P=1$ if the field is initially static and $P=2$ otherwise. Furthermore, Price showed that the perturbations of any zero rest-mass, integer-spin field are governed by a wave equation with the same qualitative form as that governing the scalar field. This suggests that the results for the scalar field should apply equally well to the radiatable multipoles of both the electromagnetic and gravitational fields. Similar results for a massless scalar field propagating on a Reissner–Nordström background have been obtained by Bičák [4]. No such analytic result has yet been obtained for the case of a black hole with angular momentum, though Krivan, Laguna, and Papadopoulos [5] have recently performed numerical work which suggests the power-law tail holds independently of the angular momentum of the black hole.

While test-field calculations are extremely compelling, it is natural to ask to what extent linear analyses are representative of dynamical gravitational collapse. If either quasinor-

mal ringing, or radiative tails, should be absent in nonlinear collapse one might view results of linear analyses with skepticism. Advances in numerical relativity make it possible to address this issue in the spherically symmetric context. Gómez and Winicour [6] studied the nonlinear evolution of a self-gravitating, spherically symmetric, massless scalar field concluding that the scalar monopole moment decayed exponentially rather than with the power law predicted by the linear analyses. More recently, Gundlach, Price, and Pullin [7,8] reexamined this problem. They were able to show that the frequencies of quasinormal oscillations, and decay rates of the power-law tails, found in the numerical solutions, are in good agreement with the predictions of perturbation theory (though one must go to sufficiently late times in order to see tail effects, this would, in part, explain the null result of Gómez and Winicour).

The presence, and slow decay, of wave tails at late times is a key ingredient leading to the instability of Cauchy horizons inside charged and rotating black holes. For black holes in asymptotically flat spacetime, the inverse power-law decay of perturbing fields at the event horizon has been used to provide initial data in linear [9,10] and nonlinear [11–14] studies of the black-hole interior. In particular, the form of the wave tail is largely responsible for the weakness of the mass-inflation singularity inside charged black holes [12], and is believed to have similar consequences inside rotating holes [13].

In contrast with the asymptotically flat case, perturbative [15,16] and nonlinear [18] studies indicate that the inner Cauchy horizon of charged and rotating black holes immersed in asymptotically de Sitter space can be stable. That stability persists for a finite volume of the parameter space suggests that these spacetimes violate the letter (if not the spirit) of the cosmic censorship hypothesis [19]. The nature of the radiative tail of perturbations at late times plays a major role in these analyses. Plausible arguments suggest that an exponential decay of the tails replaces the power-law behavior observed in asymptotically flat spacetimes [16,17]; however, no detailed analysis of the evolution of wave tails

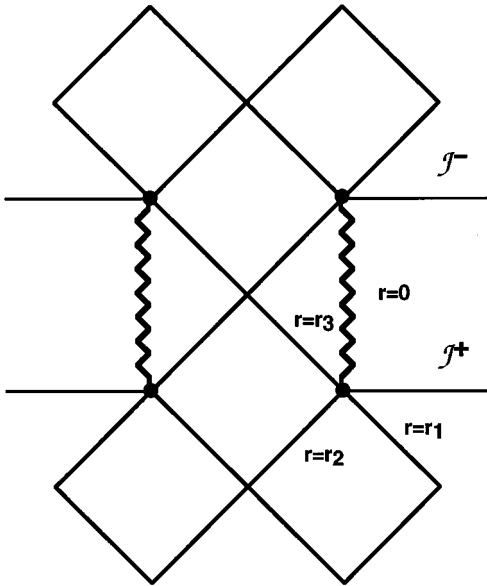


FIG. 1. A conformal diagram showing the Reissner-Nordström-de Sitter black-hole spacetime. Shown are the cosmological horizon at $r=r_1$, the black-hole event horizon at $r=r_2$, the inner (Cauchy) horizon at $r=r_3$, and the singularity (wavy line) located at $r=0$. Past and future null infinity are indicated by \mathcal{J}^- and \mathcal{J}^+ , respectively.

in asymptotically de Sitter-black-hole spacetimes exists. The present work reports on such a study for nonrotating black holes. Our primary motivation has been to obtain correct boundary conditions on the radiation at the event horizon for use in a numerical study of the internal structure of charged black holes in de Sitter space.

The paper is organized as follows: In Sec. II we consider the propagation of massless, minimally coupled scalar fields on the Schwarzschild-de Sitter and Reissner-Nordström-de Sitter black-hole backgrounds. We derive the equation governing the scalar test field, and numerically integrate it. Two independent numerical codes were used throughout the linear analysis; a null evolution scheme following that of Gundlach, Price, and Pullin [7], and a Cauchy evolution scheme similar to that described by Krivan, Laguna, and Papadopoulos [5]. We found complete agreement between them. Our results show that, except for the $\ell=0$ mode, the field falls off exponentially at the cosmological and black-hole event horizons, and at future timelike infinity. The rate of decay depends upon the surface gravity κ_1 of the cosmological horizon [see Eq. (2.4)], and the multipole order of the field. In particular, as $t \rightarrow \infty$, we find that

$$\phi \sim e^{-\ell \kappa_1 t}, \quad \ell > 0, \quad (1.1)$$

where t is defined by Eq. (2.1). When $\ell=0$, the field, rather than decaying, approaches a constant value at late times. A suggestion of this behavior can be found in the analysis of Chambers and Moss [17] and, as argued there, is similar to the case of scattering inside a charged black hole [10]. A theoretical justification of this result is presented in the Appendix. In particular, the analysis demonstrates how the con-

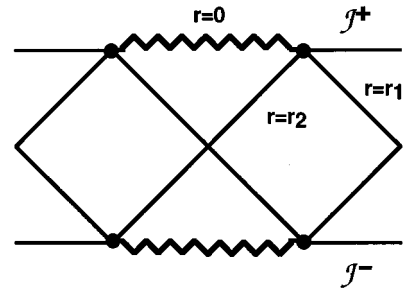


FIG. 2. A conformal diagram representing the Schwarzschild-de Sitter black-hole spacetime. Shown are the cosmological horizon at $r=r_1$, the black-hole event horizon at $r=r_2$, and the singularity (wavy line) located at $r=0$. Also shown are the locations of past and future null infinity \mathcal{J}^- and \mathcal{J}^+ , respectively.

stant part of the field scales with Λ and illustrates the independence of this scaling upon the initial data.

In Sec. III, we study the nonlinear evolution of a spherically symmetric, self-gravitating scalar field by numerically integrating the coupled Einstein-scalar field equations. Confining attention to spherical symmetry implies we gain information solely about the $l=0$ mode of the field. We find, in accord with our linear analysis, that the field approaches a constant value at the cosmological event horizon, the black-hole event horizon, and future timelike infinity, demonstrating that the results of our linear analysis are indicative of the full theory. In addition to this, we inspect the behavior of the field's stress energy, showing that

$$\phi_{,r} \sim e^{-2ku}, \quad (1.2)$$

with $k \simeq \kappa_1$ to within about 12%. In Sec. IV we make some final comments about the implications of our results for Cauchy horizon stability in black-hole-de Sitter spacetimes and the related issue of cosmic censorship.

II. A LINEAR ANALYSIS

In this section, we consider a massless, minimally coupled, scalar field propagating on a fixed Reissner-Nordström-de Sitter background. Since our considerations are limited to the black-hole exterior, it is clear that the Schwarzschild-de Sitter case can always be obtained by setting the charge $q=0$ (when this fails, we explicitly include the corresponding formulas).

A. The equations

The generalization of the Reissner-Nordström metric to include a cosmological constant was first given by Carter [20] as

$$ds^2 = -f(r)dt^2 + f(r)^{-1}dr^2 + r^2(d\theta^2 + \sin^2\theta d\phi^2), \quad (2.1)$$

where

$$f(r) = 1 - \frac{2M}{r} + \frac{q^2}{r^2} - \frac{r^2}{\alpha^2}, \quad \alpha^2 = \frac{3}{\Lambda} > 0. \quad (2.2)$$

In Eq. (2.2), M denotes the mass of the black hole, q its charge, and Λ is the cosmological constant. If $q \neq 0$ there are three horizons located at the roots of $f(r)=0$; an inner (Cauchy) horizon at $r=r_3$, a black-hole event horizon at

$r=r_2$, and a cosmological horizon located at $r=r_1$ such that $r_1 > r_2 > r_3$ (see Fig. 1). The fourth root r_4 is negative and thus nonphysical. [When $q=0$ there are only two horizons (see Fig. 2), the black-hole event horizon r_2 and the cosmological event horizon r_1 while the third root r_3 is negative.] It is convenient to introduce a ‘‘tortoise’’ radial coordinate, $r_* = \int dr/f(r)$, which takes the explicit form

$$r_* = \begin{cases} -\frac{1}{2\kappa_1} \ln \left| \frac{r}{r_1} - 1 \right| + \frac{1}{2\kappa_2} \ln \left| \frac{r}{r_2} - 1 \right| - \frac{1}{2\kappa_3} \ln \left| \frac{r}{r_3} - 1 \right| + \frac{1}{2\kappa_4} \ln \left| \frac{r}{r_4} - 1 \right|, & q \neq 0, \\ -\frac{1}{2\kappa_1} \ln \left| \frac{r}{r_1} - 1 \right| + \frac{1}{2\kappa_2} \ln \left| \frac{r}{r_2} - 1 \right| + \frac{1}{2\kappa_3} \ln \left| \frac{r}{r_3} - 1 \right|, & q = 0, \end{cases} \quad (2.3)$$

where the arbitrary constant of integration has been set to zero. We define

$$\kappa_i = \frac{1}{2} \left| \frac{df(r)}{dr} \right|_{r=r_i}, \quad (2.4)$$

where r_i are the roots of $f(r)=0$. When the root corresponds to a physical horizon in the spacetime, κ_i is the surface gravity of that horizon [21]. Finally, we introduce a pair of null coordinates on the spacetimes, the advanced time $v = t + r_*$, and the retarded time $u = t - r_*$, in terms of which the interval (2.1) reduces to

$$ds^2 = -f(r) du dv + r^2 (d\theta^2 + \sin^2 \theta d\phi^2). \quad (2.5)$$

The definition we have adopted means that the future cosmological horizon $r=r_1$ is located at $v=\infty$, and the future black-hole event horizon $r=r_2$ is at $u=\infty$. In terms of the null coordinates (u, v) , the scalar wave equation, $\square \phi = 0$, becomes

$$\Psi_{,uv} = -\frac{1}{4} V_{\ell}(r) \Psi, \quad (2.6)$$

where we have decomposed the field ϕ into its constituent multipole pieces, i.e., $\phi = \sum \Psi(u, v) Y_{\ell m}(\theta, \phi) r^{-1}$. The effective potential

$$V_{\ell}(r) = f(r) \left(\frac{\ell(\ell+1)}{r^2} + \frac{2M}{r^3} - \frac{2q^2}{r^4} - \frac{2}{\alpha^2} \right) \quad (2.7)$$

is highly localized near $r_*=0$, falling off exponentially in r_* at both $r=r_1$ and $r=r_2$. The form of the potential for $\ell=0, 1, 2$ is shown in Fig. 3.

B. The results

It is straightforward to integrate Eq. (2.6) on a null grid using the methods described by Gundlach, Price, and Pullin [7]. Further details can be found in their article.

Since tail effects are independent of the initial data used,¹ we represent a generic initial perturbation by a Gaussian pulse on $u=0$

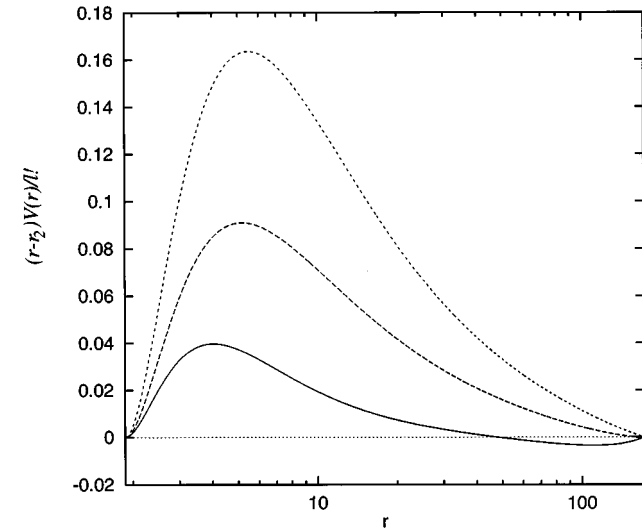


FIG. 3. The ‘‘effective’’ potential when $q=0.5$, $M=1$, $\Lambda=10^{-4}$, and $\ell=0$ (solid), $\ell=1$ (dashed), and $\ell=2$ (dotted). We have multiplied by $|r-r_2|/\ell!$ in order to accentuate the nature of the potential when $\ell=0$, the usual potential barrier is followed by a potential well, a feature not evident when $\ell>0$. The potential tends to zero exponentially quickly as $r_* \rightarrow \pm\infty$.

¹We have confirmed this in our case by using three different initial field configurations: (i) a Gaussian pulse on $u=0$ with constant field on $v=0$, (ii) a Gaussian pulse on $v=0$ with constant field on $u=0$, and (iii) a pulse on $u=0$ for which the average $\int_0^\infty \Psi(0, v) dv$ vanishes.

$$\Psi(u=0,v) = A \exp\{-(v-v_1)^2/\sigma^2\}. \quad (2.8)$$

[The amplitude A is irrelevant since Eq. (2.6) is linear. The data used to produce the figures had center $v_1=50.0$, and width $\sigma=3.0$.] The field is constant on $v=0$, $\Psi(v=0)=\Psi(u=0,v=0)$. We have set the mass of the hole M equal to unity throughout; this corresponds to the freedom to rescale the coordinates by an overall length scale. Investigations have shown that the results are qualitatively similar for all $\Lambda>0$, so we fix $\Lambda=10^{-4}$ from here on. We discuss the behavior of the field, $\phi=\Psi/r$, in three regions: (a) time-like infinity, approached on surfaces of constant r . (b) The cosmological horizon, in practice, approximated by the null surface $v=v_{\max}$, the largest value of v on our grid. (c) The black-hole event horizon, again, approximated by the null surface $u=u_{\max}$, the largest value of u on our grid.

Gundlach, Price, and Pullin [7] argued that the nature of the tails in asymptotically flat spacetimes is primarily due to the power-law form of the effective potential as $r_* \rightarrow \infty$. In asymptotically de Sitter spacetimes the effective potential is exponentially suppressed as $r_* \rightarrow \pm\infty$, therefore, it should not be surprising that the tails fall off exponentially with time. An unexpected feature of the evolution is that the $\ell=0$ mode does not decay to zero, rather a generic perturbation leads to a residual constant field at late times. (Of course, there is no stress energy associated with a constant field.) This was alluded to in a paper by Chambers and Moss [17] where it was argued that the situation in Schwarzschild–de Sitter spacetime is somewhat analogous to scattering inside a charged black hole [10], and hence a constant mode can be transmitted to both the black-hole and cosmological event horizons. Indeed, at late times we find

$$\phi|_{t=0} \simeq \phi_0 + \phi_1(r) e^{-2\kappa_1 t}. \quad (2.9)$$

Figure 4 demonstrates this effect. After a period of quasinormal ringing, whose explicit features we are not currently interested in, the field rapidly approaches the same constant value at the cosmological event horizon, the black-hole event horizon, and future timelike infinity. One might suspect that the existence of a nonzero field at late times is an artifact of the initial data, or that setting $q=0$ might produce different results. Therefore, Fig. 5 shows results for a Schwarzschild–de Sitter black hole when $\ell=0$. Once again, the field settles down to a constant value which is independent of the radial position. Monitoring the behavior of $\phi_{,t}$ during the evolution (this is a matter of formality in the Cauchy code, as it uses momenta $p_t = \phi_{,t}$ for the evolution) has allowed us to conclude that the numerical value of the exponent in Eq. (2.9) is indeed κ_1 to within 10%. In general, the final field value ϕ_0 is a function of the black-hole parameters (M, q, Λ) . Employing arguments similar to those used by Gundlach, Price, and Pullin [7], to study power-law tails in asymptotically flat black-hole spacetimes, one can show that the constant part of the field scales as $\phi_0 \sim \Lambda$ (see the Appendix). We have numerically investigated the dependence of ϕ_0 on the cosmological constant Λ and, as shown in Fig. 6 for the case when $q=0$ and $M=1$, our results indicate that $\phi_0 \sim \Lambda^{0.9994}$.

A calculation, identical to that of Gürsel *et al.* [10] for wave propagation in the interior of a Reissner–Nordström

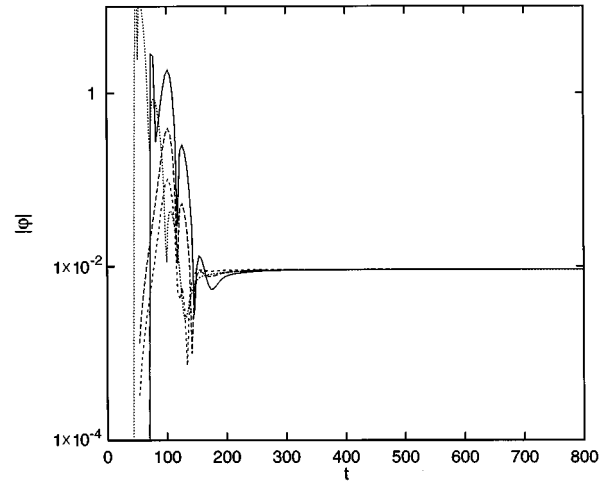


FIG. 4. The magnitude of the field $|\phi|$ versus time for $q=0.5$, $\ell=0$, $M=1$, and $\Lambda=10^{-4}$. The field is shown on the cosmological event horizon r_1 (short dashed), the black-hole event horizon r_2 (dotted), and two surfaces of constant radius (solid and long dashed). Initially the quasinormal ringing dominates, while at late times the field settles down to the same constant value on all four surfaces.

black hole, reveals that the zero frequency reflection and transmission coefficients for the $\ell=0$ mode, in the exterior of Schwarzschild–de Sitter and Reissner–Nordström–de Sitter black holes, are given by

$$R = \frac{(r_1^2 - r_2^2)^2}{(r_1^2 + r_2^2)^2}, \quad T = \frac{4r_1^2 r_2^2}{(r_1^2 + r_2^2)^2}. \quad (2.10)$$

One should contrast the nonzero value of the transmission coefficient T , in this case, with the results for scattering in the exterior of asymptotically flat black-hole spacetimes [3]. In that case the transmission coefficients are of order $\omega^{\ell+1}$ for small ω and, consequently, the constant modes are trapped [1].

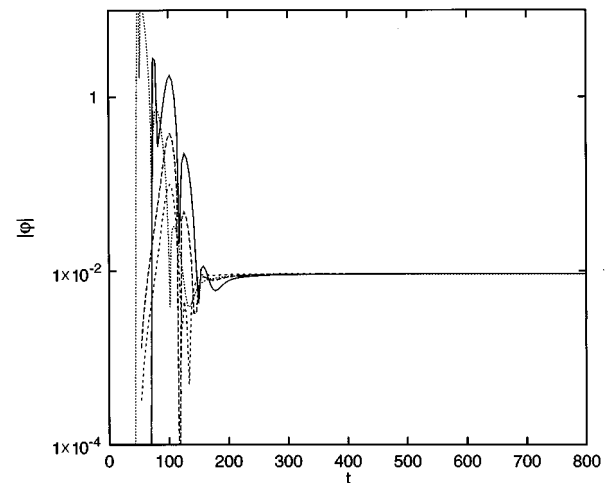


FIG. 5. A plot of $|\phi|$ versus time when $q=0.0$, $\ell=0$, $M=1$, and $\Lambda=10^{-4}$. The field is exhibited on the same surfaces as the $q=0.5$ cases. Once again, the asymptotically constant field is evident.

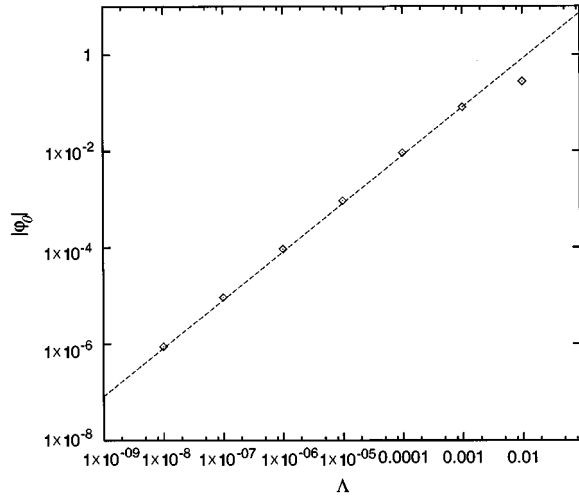


FIG. 6. The asymptotic value of the field $|\phi_0|$ versus Λ for evolutions with $q=0.0$, $\ell=0$, and $M=1$. The dashed line represents the least square fit to $\ln|\phi_0|=b+a\ln|\Lambda|$ with $a=1.02$, $b=4.65$. The linear correlation coefficient c_{lin} of $\ln|\phi_0|$ versus $\ln\Lambda$ is given by $c_{\text{lin}}=0.999$.

For $\ell>0$ the picture is different, as seen in Figs. 7 and 8. The early time behavior of the field is still dominated by complicated quasinormal ringing, but at late times a definite exponential falloff is manifest. In particular, the late time wave tails are well approximated by $|\phi|_{\ell} \sim \exp(-\ell\kappa_1 t)$. In a series of separate evolutions we found that for sufficiently small values of Λ , a regime of power-law decay followed the quasinormal ringing, though at late times the exponential decay described above always dominates.

III. NONLINEAR ANALYSIS

Given the somewhat unusual behavior of the $\ell=0$ mode elucidated by the test-field analysis, it seems necessary to examine the nonlinear evolution of a self-gravitating mass-

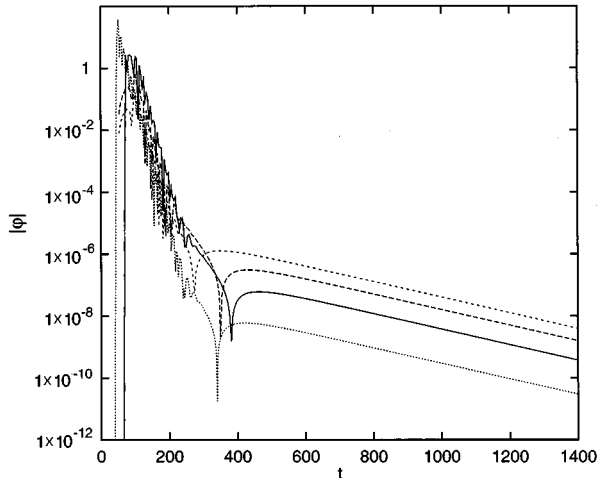


FIG. 7. A plot of $|\phi|$ versus time for $q=0.5$, $\ell=1$, $M=1$, and $\Lambda=10^{-4}$. The field along is shown on the cosmological event horizon r_1 (short dashed), the black-hole event horizon r_2 (dotted), and two surfaces of constant radius (solid and long dashed). The field falls off as $\exp(-kt)$ at late times, with $k \approx \kappa_1$ to within about 2%. Note that the ordinate scale is logarithmic.

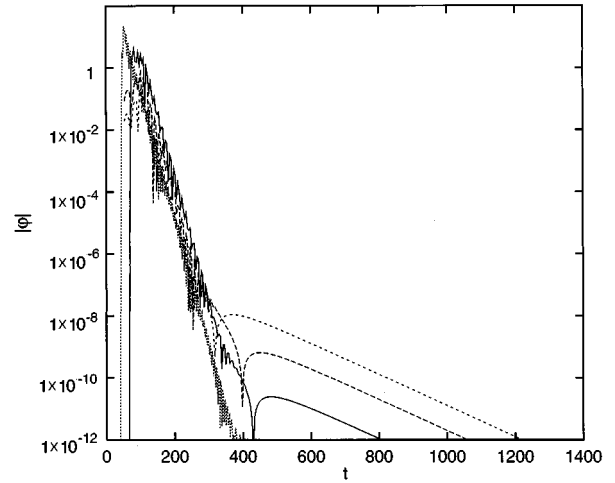


FIG. 8. A plot of $|\phi|$ versus time for $q=0.5$, $\ell=2$, $M=1$, and $\Lambda=10^{-4}$. The field is shown on the cosmological event horizon r_1 (short dashed), the black-hole event horizon r_2 (dotted), and two surfaces of constant radius (solid and long dashed). At early times quasinormal ringing completely dominates, but eventually the field falls off as $\exp(-2kt)$. The value of $k \approx \kappa_1$ is again accurate to approximately 2%. Note that the ordinate scale is logarithmic.

less, scalar field in the presence of a cosmological constant. This situation is described by the coupled Einstein-scalar field equations

$$G_{\alpha\beta} = 8\pi T_{\alpha\beta} - g_{\alpha\beta}\Lambda, \quad (3.1)$$

where

$$T_{\alpha\beta} = \phi_{,\alpha}\phi_{,\beta} - (1/2)g_{\alpha\beta}(\phi_{,\gamma}\phi^{,\gamma}), \quad (3.2)$$

is the stress energy of the scalar field which satisfies $\square\phi=0$. Restricting attention to spherical symmetry (thus we only gain information about the $\ell=0$ mode), the line element can be written as

$$ds^2 = -g\bar{g}du^2 - 2gdudr + r^2(d\theta^2 + \sin^2\theta d\phi^2), \quad (3.3)$$

where $g=g(u,r)$, $\bar{g}=\bar{g}(u,r)$, and u is the retarded time. The coordinates have been normalized so that u is the proper time at the origin, thus $g(u,0)=\bar{g}(u,0)=1$. It is customary [23] to introduce two new fields $\bar{h}(u,r)$ and $h(u,r)$ defined by

$$\phi = \bar{h} = \frac{1}{r} \int_0^r h dr. \quad (3.4)$$

In terms of these variables the field equations (3.1) become

$$(\ln g)_{,r} = 4\pi r^{-1}(h - \bar{h})^2, \quad (3.5)$$

$$(r\bar{g})_{,r} = g(1 - \Lambda r^2), \quad (3.6)$$

$$(r\bar{h})_{,r} = h, \quad (3.7)$$

and the wave equation is

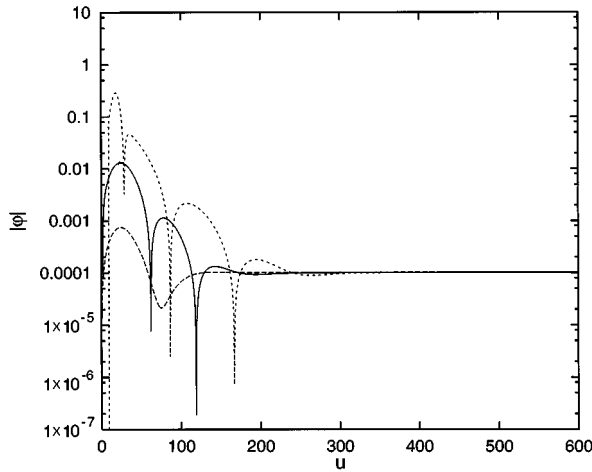


FIG. 9. A plot of $|\phi|$ versus time for $\Lambda = 10^{-4}$. The field is shown along three surfaces: the cosmological event horizon r_1 (short dashed), the black-hole event horizon r_2 (long dashed), and a surface of constant radius (solid). After a period of quasinormal ringing the field settles down to the same constant value at all three surfaces.

$$h_{,u} - \frac{\bar{g}}{2} h_{,r} = \frac{(h - \bar{h})}{2r} [g(1 - \Lambda r^2) - \bar{g}]. \quad (3.8)$$

A well-established numerical algorithm exists to integrate these equations [8,24,25]. We refer the reader to these articles for details.

Initial data for the nonlinear equations is supplied on an initial null cone centered on the origin. We considered a Gaussian pulse on $u=0$, with an amplitude $\phi_0(r/r_0)^2$, width σ , and centered on $r=r_0$. The code was tested against the exact solution in [26]. We also reproduced power-law tails in complete agreement with [8], when $\Lambda=0$.

Figure 9 shows \bar{h} (or equivalently ϕ) at the cosmological event horizon, the black-hole event horizon, and along an $r=\text{const}$ surface. The agreement with the linear analysis is remarkable. We again see an initial period of quasinormal ringing which decays, leaving behind a constant field at late times.

Furthermore, using Eqs. (3.4) and (3.7) we can write $r\phi_{,r} = (\bar{h} - h)$ and examine the stress energy of the field at late times. Figure 10 suggests that $(\bar{h} - h) \sim \exp[-2\kappa_1 u]$ at late times, as suggested by the test-field analysis.

IV. CONCLUDING REMARKS

This study of wave-tail evolution in black-hole–de Sitter spacetimes has revealed consistent but interesting results. The radiative tails associated with a massless, minimally coupled scalar field propagating on the fixed backgrounds of a Schwarzschild–de Sitter and Reissner–Nordström–de Sitter black hole decay exponentially at the cosmological horizon, the black-hole event horizon, and at future timelike infinity. This result is not too surprising when one considers the conclusions of Ching *et al.* [22], who have demonstrated that the usual inverse power-law tails, as seen in asymptotically flat black-hole spacetimes, are not a generic feature of wave propagation in curved spacetime. An unusual feature of

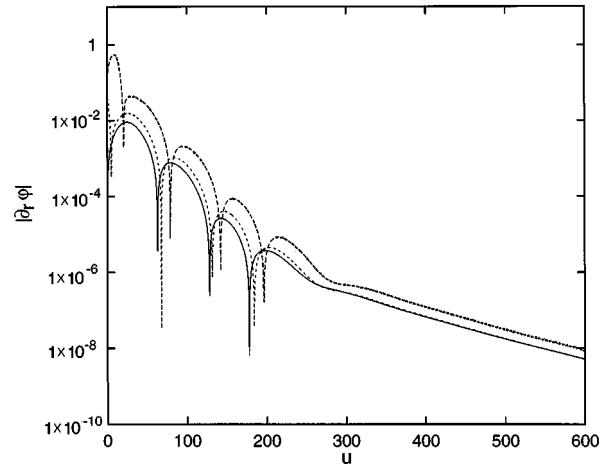


FIG. 10. The derivative of the field $|\phi_{,r}|$ versus time along three surfaces: the cosmological event horizon r_1 (short dashed), the black-hole event horizon r_2 (long dashed), and a surface of constant radius (solid). The nonlinear evolution had $\Lambda = 10^{-4}$. At late times exponential decay with the approximate form $\exp(-2ku)$ is evident, we have determined the value of $k \approx \kappa_1$ within about 12%.

the analysis is the behavior of the $\ell=0$ mode. We have seen that, rather than decaying, the $\ell=0$ mode approaches a constant value at late times. Motivated by this result, we considered the nonlinear problem of a scalar field coupled to gravity and numerically integrated the Einstein-scalar field equations. These results show excellent agreement with the linear analysis. In addition, an analytic investigation of scattering in the exterior of black-hole–de Sitter spacetimes has allowed us to predict that the constant mode scales as $\phi_0 \sim \Lambda$, independently of the initial data, and agreeing completely with the results of our numerical study. In particular, we have been able to show that the zero frequency reflection and transmission coefficients for the $\ell=0$ mode are nonzero and, unlike the situation in asymptotically flat black-hole spacetimes, the constant modes can be propagated throughout the exterior.

Though the introduction of a nonzero cosmological constant into the Einstein equations may be argued to be somewhat unrealistic, it is the issue of Cauchy horizon stability in black-hole–de Sitter spacetimes [15,16] and the related issue of cosmic censorship [19], that motivates this investigation. The power-law tails found by Price [3] have been used as initial data in arguments pertaining to the instability of the inner (Cauchy) horizon of both the Reissner–Nordström and Kerr black-hole spacetimes and the associated phenomenon of mass inflation. Linear perturbation studies suggest that the Cauchy horizon inside black holes embedded in de Sitter space may be stable, fluxes of linear perturbations remain bounded at the Cauchy horizon. This in itself does not guarantee stability though. A fully nonlinear analysis of the black-hole interior is needed, for which the late-time wave tails at the event horizon serve as initial data. With the results of this paper in hand, we can now embark on a numerical study of the Cauchy horizon in Reissner–Nordström–de Sitter, along the lines of Brady and Smith [14].

ACKNOWLEDGMENTS

P.R.B. is grateful to Bruce Allen and Kip Thorne for helpful discussions. C.M.C. wishes to thank the Caltech Relativ-

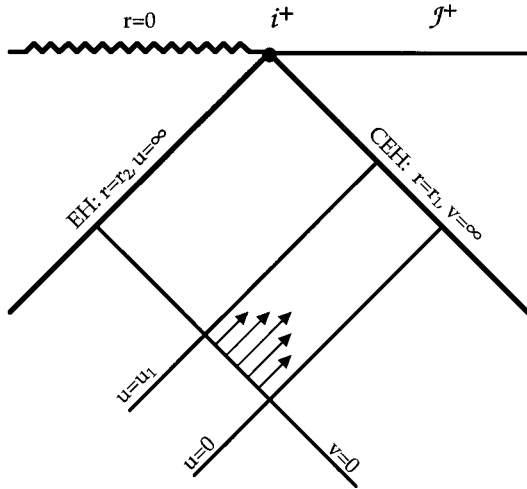


FIG. 11. The region of spacetime important for scattering between the black-hole event horizon (EH), and the cosmological event horizon (CEH) of a black hole in de Sitter space. We consider an initial burst of radiation on $v=0$ which is confined between the two null lines $u=0$ and $u=u_1$. The analysis in the Appendix considers the evolution of the field in the diamond-shaped region determined by $0 \leq u < \infty$ and $0 \leq v < \infty$. We find that the $\ell=0$ mode of the scalar field settles down to a constant, nonzero value at the EH, the CEH, and timelike infinity.

ity Group for hospitality during the completion of this work and the Relativity group at Montana State University for their constant support over the last year. C.M.C. thanks The Royal Commission For The Exhibition Of 1851 whose financial support is gratefully acknowledged. P.R.B. was supported by the PMA at Caltech and the NSF Grant No. AST-9417371. W.K. was supported by the Deutscher Akademischer Austauschdienst (DAAD). P.L. was supported by the Binary Black Hole Grand Challenge Alliance, NSF PHY/ASC 9318152 (ARPA supplemented) and by NSF Grant Nos. PHY 96-01413 and 93-57219 (NYI).

APPENDIX: LATE-TIME BEHAVIOR OF THE $\ell=0$ MODE

Price [3] has shown that a scalar field ϕ in the exterior of an asymptotically flat black hole decays to zero at late times, provided the initial data has compact support. Here, we consider scattering of the $\ell=0$ mode between the cosmological and black-hole event horizons in Schwarzschild–de Sitter spacetime. (The results extend easily to include charge.) While the qualitative features of this analysis should hold for all values of Λ , we make the assumption that the cosmological constant is sufficiently small that we can approximate the radius of the cosmological horizon by $r_1 \approx \sqrt{3/\Lambda}$. Following Gundlach, Price, and Pullin [7], we break the evolution up into two parts: (i) the evolution of an initial burst $\Psi(u,0)=G(u)$, for which $G(u) \neq 0$ only when $0 < u < u_1$, and $\Psi(0,v) \equiv 0$, and (ii) the subsequent evolution of the field for $u \geq u_1$. This situation is indicated in Fig. 11.

When $\ell=0$, the general solution to Eq. (2.6) can be written as a series depending on two arbitrary functions $F(v)$ and $G(u)$; thus,

$$\Psi = A[G(u) + F(v)] + \sum_{p=0}^{\infty} B_p(r)[G^{(-p-1)}(u) + (-1)^{(p+1)}F^{(-p-1)}(v)], \quad (\text{A1})$$

where negative superindices refer to integration with respect to the argument of the function. The coefficient A is set equal to unity, without loss of generality, while the $B_p(r)$ satisfy the recurrence relation

$$B'_{p+1} = \left(\frac{M}{r^3} - \frac{\Lambda}{3}\right)(rB'_p - B_p) + fB''_p/2. \quad (\text{A2})$$

Here a prime indicates differentiation with respect to r , and B_0 is given by

$$B_0 = \frac{M}{2r^2} + \frac{\Lambda r}{3}. \quad (\text{A3})$$

The first part of the evolution, scattering of the initial pulse $G(u)$ in the region $0 < u < u_1$, implies that the field on $u = u_1$ is given by

$$\Psi(u_1, v) = \sum_{p=0}^{\infty} B_p(r)G^{(-p-1)}(u_1), \quad (\text{A4})$$

since $G(u_1) = 0$. It is straightforward to show that the coefficients $B_p(r)$ do not vanish as $r_* \rightarrow \infty$, corresponding to the cosmological horizon and, in this limit, the field is nonzero for generic initial data. In asymptotically flat space this limit is equivalent to $r \rightarrow \infty$, and all of the $B_p(r)$ vanish; this is the central difference between our analysis and that of Price [3]. Moreover, for sufficiently small Λ the value of Ψ on the cosmological horizon is given by

$$\Psi(u_1, \infty) \approx \sqrt{\Lambda/3} \int_0^{u_1} G(u) du + O(\Lambda). \quad (\text{A5})$$

We can now examine the evolution of the field in the region $u \geq u_1$ using Eq. (A4) as initial data; it is at this point that our argument deviates from that of Gundlach, Price, and Pullin [7]. For sufficiently small values of Λ , and $\ell=0$, we can solve Eq. (2.6) near to the cosmological horizon by neglecting the mass of the black hole; the solution is simply

$$\Psi \approx (\Lambda r/3)[g(u) + f(v)] + [\partial_u g(u) - \partial_v f(v)], \quad (\text{A6})$$

where $g(u)$ and $f(v)$ are arbitrary functions. We can determine $f(v)$ by matching it to the initial data in Eq. (A4), thus, near the cosmological horizon, and by virtue of the relation $r_* = (v - u)/2$, we have

$$f(v) = f_0 + \sum_{n=1}^{\infty} f_n e^{-n\kappa_1 v}, \quad (\text{A7})$$

where $f_0 = 3\Psi(u_1, \infty)/(\Lambda r_1)$. The precise form of $g(u)$ depends on the nature of the potential *everywhere*, however, since it develops from the field configuration given in Eq. (A4) it seems reasonable to assume that it can be written as

$$g(u) = g_0 + \sum_{n=1}^{\infty} g_n e^{-n\kappa_1 u}, \quad (\text{A8})$$

when $u \rightarrow \infty$. In this way, we conclude that a generic perturbation will lead to a constant value for the field $\phi = \Psi/r$ at late times, provided $f_0 \neq g_0$. When $\ell = 0$, this is the only static solution which is regular at both horizons. Finally, we note that the final value of the field ϕ_0 in Eq. (2.9) scales as

$$\phi_0 \sim \Lambda \quad (\text{A9})$$

for small values of Λ . This is confirmed by the numerical results in Sec. IIB.

-
- [1] C.W. Misner, K.S. Thorne, and J.A. Wheeler, *Gravitation* (Freeman, San Francisco, 1973).
- [2] K.S. Thorne, in *300 Years of Gravitation*, edited by S.W. Hawking and W. Israel (Cambridge University Press, Cambridge, England, 1987).
- [3] R.H. Price, Phys. Rev. D **5**, 2419 (1972); **5**, 2439 (1972).
- [4] J. Bičák, Gen. Relativ. Gravit. **3**, 331 (1972).
- [5] W. Krivan, P. Laguna, and P. Papadopoulos, Phys. Rev. D **54**, 4728 (1996).
- [6] R. Gómez and J. Winicour, J. Math. Phys. (N.Y.) **33**, 1445 (1992).
- [7] C. Gundlach, R.H. Price, and J. Pullin, Phys. Rev. D **49**, 883 (1994).
- [8] C. Gundlach, R.H. Price, and J. Pullin, Phys. Rev. D **49**, 890 (1994).
- [9] S. Chandrasekhar and J.B. Hartle, Proc. R. Soc. London **A284**, 301 (1982); M. Simpson and R. Penrose, Int. J. Theor. Phys. **7**, 183 (1973).
- [10] Y. Gürsel, V.D. Sandberg, I.D. Novikov, and A.A. Starobinsky, Phys. Rev. D **19**, 413 (1979); **20**, 1260 (1979).
- [11] W. Israel and E. Poisson, Phys. Rev. D **41**, 1796 (1990); A. Bonnano, S. Droz, W. Israel, and S.M. Morsink, Can. J. Phys. **72**, 755 (1994), and references therein.
- [12] A. Ori, Phys. Rev. Lett. **67**, 789 (1991); R. Balbinot, P.R. Brady, E. Poisson, and W. Israel, Phys. Lett. A **161**, 223 (1991).
- [13] A. Ori, Phys. Rev. Lett. **68**, 2117 (1992); P.R. Brady and C.M. Chambers, Phys. Rev. D **51**, 4177 (1995); P.R. Brady, S. Droz, W. Israel, and S.M. Morsink (unpublished).
- [14] P.R. Brady and J.D. Smith, Phys. Rev. D **75**, 1256 (1995).
- [15] F. Mellor and I.G. Moss, Phys. Rev. D **41**, 403 (1990); Class. Quantum Grav. **9**, L43 (1992); C.M. Chambers and I.G. Moss, *ibid.* **11**, 1035 (1994).
- [16] P.R. Brady and E. Poisson, Class. Quantum Grav. **9**, 121 (1992).
- [17] C.M. Chambers and I.G. Moss, Phys. Rev. Lett. **73**, 617 (1994).
- [18] P.R. Brady, D. Núñez, and S. Sinha, Phys. Rev. D **47**, 4239 (1993).
- [19] See R. Penrose, in *Battelle Rencontres*, edited by C.M. DeWitt and J.A. Wheeler (Benjamin, New York, 1968), for a discussion on the relationship between Cauchy horizon instability and the cosmic censorship hypothesis.
- [20] B. Carter, in *Black Holes*, edited by C.M. DeWitt and B.S. DeWitt (Gordon and Breach, New York, 1973).
- [21] R.M. Wald, *General Relativity* (University of Chicago Press, Chicago, 1984), Chap. 12.
- [22] E.S.C. Ching, P.T. Leung, W.M. Suen, and K. Young, Phys. Rev. Lett. **74**, 2414 (1995).
- [23] D. Christodoulou, Commun. Math. Phys. **105**, 337 (1986).
- [24] D.S. Goldwirth and T. Piran, Phys. Rev. D **36**, 3575 (1987).
- [25] D. Garfinkle, Phys. Rev. D **51**, 5558 (1995).
- [26] P.R. Brady, Class. Quantum Grav. **11**, 1255 (1994).